

Nonvolatile resistive switching in $\text{Pr}_{0.7}\text{Ca}_{0.3}\text{MnO}_3$ devices using multilayer graphene electrodes

Wootae Lee,^{1,a)} Gunho Jo,¹ Sangchul Lee,² Jubong Park,¹ Minseok Jo,¹ Joonmyoung Lee,¹ Seungjae Jung,¹ Seonghyun Kim,¹ Junggho Shin,¹ Sangsu Park,² Takhee Lee,^{1,2} and Hyunsang Hwang^{1,2,b)}

¹School of Materials Science and Engineering, Gwangju Institute of Science and Technology (GIST), 261 Cheomdan-Gwagi-ro (Oryong-dong), Buk-gu, Gwangju 500-712, Republic of Korea

²Department of Nanobio Materials and Electronics (WCU), Gwangju Institute of Science and Technology (GIST), 261 Cheomdan-Gwagi-ro (Oryong-dong), Buk-gu, Gwangju 500-712, Republic of Korea

(Received 9 October 2010; accepted 30 December 2010; published online 20 January 2011)

We report resistive switching in $\text{Pr}_{0.7}\text{Ca}_{0.3}\text{MnO}_3$ (PCMO) devices using multilayer graphene (MLG) for nonvolatile memory applications. When MLG was used as a conducting electrode, PCMO device exhibited resistive switching with an on/off ratio of over two orders of magnitude and stable retention characteristics for over 10^4 s at 85 °C. Raman spectroscopy in both resistance states revealed increases in D and D' peaks associated with defects and large shift in G peak position for high-resistance state. This was attributed to formation and dissolution of oxygenated graphene at the MLG/PCMO interface, resulting in resistive switching. © 2011 American Institute of Physics. [doi:10.1063/1.3544051]

Resistance random access memory (RRAM) is promising for next-generation nonvolatile memory because of its simple structure, low power consumption, fast switching speed, and ease of fabrication.¹ Among various materials exhibiting resistive switching,² $\text{Pr}_{0.7}\text{Ca}_{0.3}\text{MnO}_3$ (PCMO), especially in combination with a reactive metal,³ can be used to realize excellent resistive switching properties such as good device uniformity, high endurance, and stable retention characteristics.⁴ Previous studies on reactive metal/PCMO devices revealed that oxygen ions in PCMO move to oxidize a reactive metal under an electric field, resulting in resistive switching.⁴

Recently, graphene, a two-dimensional material having a honeycombed carbon nanostructure, has attracted considerable attention because of its applications to conducting electrodes in solar cells,⁵ field-effect transistors,⁶ and light-emitting diodes.⁷ Its high transparency, high flexibility, and low sheet resistance make it suitable for use as a conducting electrode.⁵⁻⁷ Graphene can be functionalized by oxygen-related groups such as epoxides and hydroxyls, resulting in modified structural and electronic properties.⁸ In addition, its conductivity depends on oxygen-induced defects and disorders;^{9,10} that of oxygenated graphene, which is highly insulating, increases upon thermal or chemical reduction.^{11,12}

In this paper, we report resistive switching in PCMO devices using multilayer graphene (MLG) for nonvolatile memory applications. Interfacial-reaction-type resistive switching was observed upon introducing MLG as a conducting electrode to electrochemically functionalize graphene at the MLG/PCMO interface. Based on the electrical measurements and Raman spectroscopy analysis, the probable switching mechanism of our device was discussed.

After conventional cleaning of the Pt/Ti/SiO₂/Si substrate, a 60-nm-thick PCMO film was deposited by radio frequency magnetron sputtering at 450 °C. MLG films were

fabricated on nickel films, which afford high transparency, low sheet resistance, and high scalability, by chemical vapor deposition (CVD).¹³ Details of CVD-grown MLG films have been described elsewhere.⁷ After fabrication, MLG films were detached from nickel layers by etching in iron chloride (FeCl₃) solution (~1 M). The films were then transferred to the PCMO/Pt/SiO₂/Si substrate, after which the top electrode regions were protected by using a photoresist (PR) as an etch mask. Finally, the device area was patterned by O₂ plasma etching. Figure 1(a) shows a schematic diagram of MLG/PCMO/Pt. A reference PCMO device with a Pt top electrode was also fabricated.

To confirm their quality, pristine MLG films were characterized by Raman spectroscopy using a 514-nm Ar laser in ambient air, as shown in Fig. 1(b). The D-band intensity was found to be lower than the G-band one, indicating that defects and local disorders in our MLG films were small.¹⁴ In addition, sheet resistances of MLG films were measured to be $\sim 700 \pm 100 \Omega/\text{cm}^2$ by the van der Pauw four-probe method using the Hall measurement system, indicating that our films could be used as conducting electrodes in nonvolatile memory.

Figure 2(a) shows typical current-voltage characteristics of MLG/PCMO/Pt. A bias was applied to top electrode (MLG), whereas bottom electrode (Pt) was grounded, as

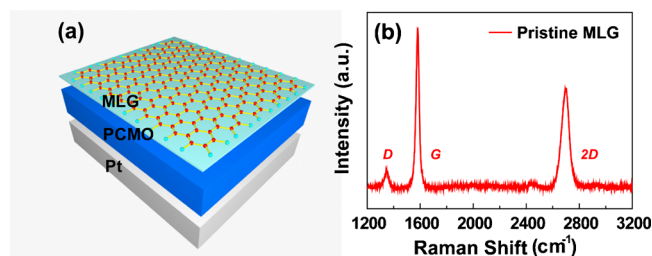


FIG. 1. (Color online) (a) Schematic diagram of PCMO device with MLG film as conducting electrode. (b) Raman spectra of pristine MLG films using 514-nm Ar laser.

^{a)}Electronic mail: rucyris@gist.ac.kr.

^{b)}Electronic mail: hwanghs@gist.ac.kr.

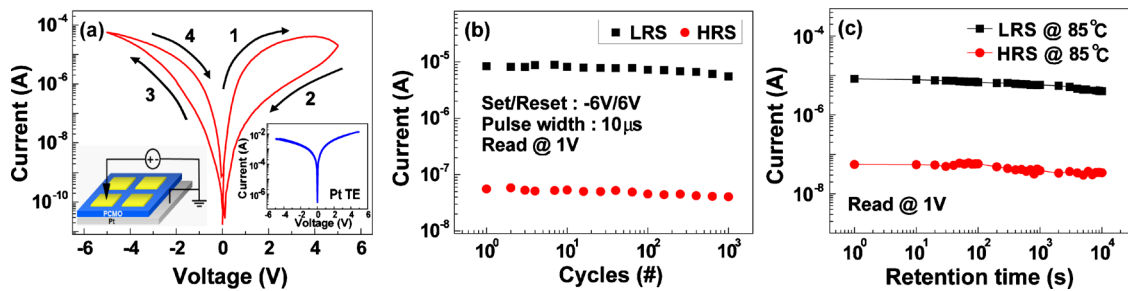


FIG. 2. (Color online) (a) Typical current-voltage curves for PCMO device with MLG electrode. The direction of dc sweep is indicated by arrows. The left inset shows the measurement configuration of the devices and the right inset, the current-voltage characteristics of PCMO device with Pt top electrode. (b) Pulse endurance and (c) retention characteristics of MLG/PCMO/Pt, indicating stable HRS and LRS for up to 10^4 s at 85°C .

shown in the left inset of Fig. 2(a). To prevent electrical breakdown of the device, we restricted the voltage from -5 V to 5 V and the direction of dc sweep was given as $1 \rightarrow 2 \rightarrow 3 \rightarrow 4$. On increasing the applied positive voltage from 0 to 5 V, the device state changed from the low-resistance state (LRS) to the high-resistance state (HRS), whereas on increasing the applied negative voltage from 0 to -5 V, LRS was obtained. Moreover, the forming process typically required to initiate a filament-type resistive memory¹⁵ was not required in our device. To compare the effect of the top electrode on resistive switching, current-voltage characteristics of a PCMO device with a Pt top electrode were also measured, as shown in the right inset of Fig. 2. Unlike with an MLG electrode, resistive switching was not observed with an inert Pt top electrode. For practical applications, we performed the pulse endurance of our device, as shown in Fig. 2(b). We applied 6 and -6 V with a $10 \mu\text{s}$ width for reset (LRS to HRS) and set (HRS to LRS) operations, respectively. The HRS and LRS show a negligible degradation for 10^3 cycles. Figure 2(c) shows the retention characteristics of our device at 85°C . After resistive switching, HRS and LRS were monitored at 1 V for 10^4 s. Stable R_{high} and R_{low} were observed and large $R_{\text{high}}/R_{\text{low}}$ ratio was maintained during measurement.

To study the effect of device size on resistive switching, the device area dependence of resistance values in HRS and LRS was investigated, as shown in Fig. 3(a). Both resistance values were inversely proportional to device area, indicating that resistive switching was not localized. In filament-type RRAM, LRS exhibited a negligible device area dependence because of the localization of the conducting path,¹⁵ whereas in interfacial-reaction-type RRAM, both HRS and LRS increased with device size.¹⁶ These results suggest that resistive switching in the MLG/PCMO/Pt device originates from reactions at the MLG/PCMO interface.

To clarify the origin of resistive switching, Raman spectroscopy analyses in both HRS and LRS were performed, as shown in Fig. 3(b). In HRS, defect-induced D and D' peaks increased significantly to around 1350 and 1620 cm^{-1} , respectively. Because these peak intensities indicate a degree of functionalization in the modified graphene structure,¹⁷ clearly, our MLG film in HRS is electrochemically modified by the electric field. This functionalization could mainly be caused by the movement of oxygen ions from PCMO under an external bias. In contrast, small D and D' band intensities were observed in LRS, indicating a decrease in defects and local disorders in the MLG film. Moreover, the G band peak shifted to a higher frequency in HRS relative to that in LRS, possibly due to MLG film oxidation.¹⁸ Figure 3(c) indicates that the G peak position and $I(\text{D})/I(\text{G})$ of MLG film in the pristine state, LRS, and HRS were 1579.5 cm^{-1} and 0.10 , 1580.6 cm^{-1} and 0.13 , and 1587.7 cm^{-1} and 1.55 , respectively.

These results suggest that resistive switching occurs in MLG/PCMO/Pt, as shown in Fig. 4. When a positive bias is applied, oxygen ions in PCMO are incorporated into the MLG and an oxygenated graphene layer is formed at the MLG/PCMO interface, as illustrated in Fig. 4(a). Therefore, the total resistance of MLG/PCMO/Pt increases and switching from LRS to HRS is achieved. Conversely, when a negative bias is applied, oxygen ions are extracted from oxygenated graphene, resulting in the dissolution of the oxygenated graphene layer at the MLG/PCMO interface. Consequently, the conductivity of oxygenated graphene increases and the device switches to the LRS, as shown in Fig. 4(b).

In summary, we have demonstrated resistive switching in a PCMO device using a multilayer graphene (MLG) electrode. A large on/off ratio greater than two orders of magnitude and stable retention characteristics for more than 10^4 s at 85°C were obtained in the MLG/PCMO/Pt device. Our

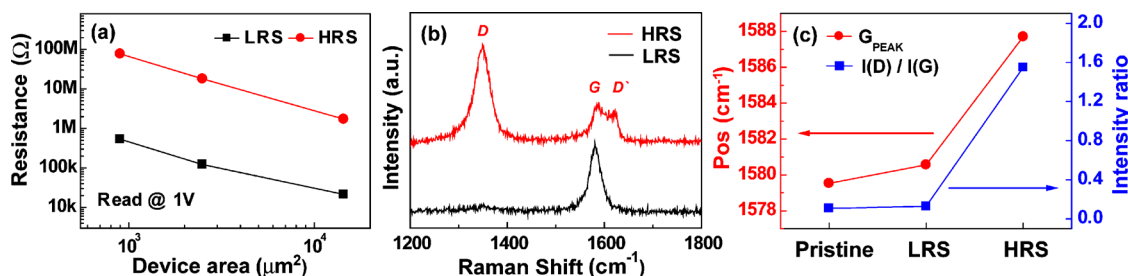


FIG. 3. (Color online) (a) Device area dependence of resistance values in HRS and LRS. (b) Comparison of Raman spectra of MLG/PCMO/Pt device in HRS and LRS, indicating sudden increase in D and D' peaks and shift of G peak position in HRS. (c) G peak position and intensity ratio of D peak to G peak in MLG films in pristine state, LRS, and HRS.

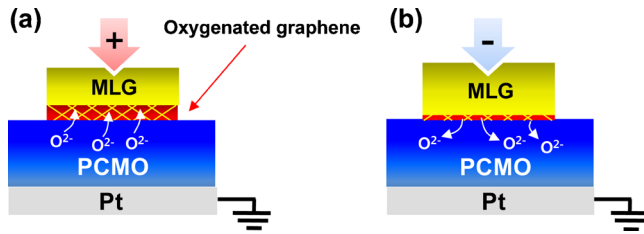


FIG. 4. (Color online) Schematic illustrations of resistive switching in MLG/PCMO/Pt device: (a) HRS and (b) LRS.

device exhibited typical interfacial-reaction-type RRAM behavior; no forming process was required and both HRS and LRS changed with device size. Moreover, Raman spectra obtained in HRS revealed sudden increases in D and D' peaks and a large shift in G band peak to a higher frequency as compared to those in LRS. These results indicate that resistive switching is attributable to formation and dissolution of an oxygenated graphene layer at the MLG/PCMO interface.

This work was supported by the National Research Program of the 0.1 Terabit Nonvolatile Memory Development Project and the National Research Laboratory (NRL) Programs of the Korea Science and Engineering Foundation (KOSEF).

¹C. Yoshida, K. Tsunoda, H. Noshiro, and Y. Sugiyama, *Appl. Phys. Lett.* **91**, 223510 (2007).

²H. Y. Lee, Y. S. Chen, P. S. Chen, T. Y. Wu, F. Chen, C. C. Wang, P. J. Tzeng, M.-J. Tsai, and C. Lien, *IEEE Electron Device Lett.* **31**, 44 (2010).

³Z. L. Liao, Z. Z. Wang, Y. Meng, Z. Y. Liu, P. Gao, J. L. Gang, H. W.

Zhao, X. J. Liang, X. D. Bai, and D. M. Chen, *Appl. Phys. Lett.* **94**, 253503 (2009).

⁴D. Seong, M. Hasan, H. Choi, J. Lee, J. Yoon, J. Park, W. Lee, M. Oh, and H. Hwang, *IEEE Electron Device Lett.* **30**, 919 (2009).

⁵X. Wang, L. Zhi, and K. Mullen, *Nano Lett.* **8**, 323 (2008).

⁶W. Liu, B. L. Jackson, J. Zhu, C. Miao, C. Chung, Y. Park, K. Sun, J. Woo, and Y. Xie, *ACS Nano* **4**, 3927 (2010).

⁷G. Jo, M. Choe, C. Cho, J. H. Kim, W. Park, S. Lee, W. Hong, T. Kim, S. Park, B. Hong, Y. H. Kahng, and T. Lee, *Nanotechnology* **21**, 175201 (2010).

⁸N. Leconte, J. Moser, P. Ordejon, H. Tao, A. Lherbier, A. Bachtold, F. Alsina, C. M. S. Torres, J. Charlier, and S. Roche, *ACS Nano* **4**, 4033 (2010).

⁹K. Kim, H. J. Park, B. Woo, K. J. Kim, G. T. Kim, and W. S. Yun, *Nano Lett.* **8**, 3092 (2008).

¹⁰D. C. Kim, D. Jeon, H. Chung, Y. Woo, J. K. Shin, and S. Seo, *Nanotechnology* **20**, 375703 (2009).

¹¹Z. Wei, D. Wang, S. Kim, S. Kim, Y. Hu, M. K. Yakes, A. R. Laracuente, Z. Dai, S. R. Marder, C. Berger, W. P. King, W. A. Heer, P. E. Sheehan, and E. Riedo, *Science* **328**, 1373 (2010).

¹²C. Gómez-Navarro, R. T. Weitz, A. M. Bittner, M. Scolari, A. Mews, M. Burghard, and K. Kern, *Nano Lett.* **7**, 3499 (2007).

¹³L. Gomez De Arco, Y. Zhang, C. W. Schlenker, K. Ryu, M. E. Thompson, and C. Zhou, *ACS Nano* **4**, 2865 (2010).

¹⁴A. C. Ferrari, J. C. Meyer, V. Scardaci, C. Casiraghi, M. Lazzeri, F. Mauri, S. Piscanec, D. Jiang, K. S. Novoselov, S. Roth, and A. K. Geim, *Phys. Rev. Lett.* **97**, 187401 (2006).

¹⁵H. Shima, F. Takano, Y. Tamai, I. H. Inoue, H. Takagi, and H. Akinaga, *Appl. Phys. Lett.* **91**, 012901 (2007).

¹⁶H. Sim, H. Choi, D. Lee, M. Chang, D. Choi, Y. Son, E. Lee, W. Kim, Y. Park, I. Yoo, and H. Hwang, *Tech. Dig. - Int. Electron Devices Meet.* **2005**, 758.

¹⁷M. Baraket, S. G. Walton, E. H. Lock, J. T. Robinson, and F. K. Perkins, *Appl. Phys. Lett.* **96**, 231501 (2010).

¹⁸L. Liu, S. Ryu, M. R. Tomasik, E. Stolyarova, N. Jung, M. S. Hybertsen, M. L. Steigerwald, L. E. Brus, and G. W. Flynn, *Nano Lett.* **8**, 1965 (2008).